Vulnerability map of the Italian study site

Deliverable D_5.2.2

Contributing partners:

PP1 – CNR IGG

TABLE OF CONTENTS

1 Introduction

This report is the project deliverable “Vulnerability map of the Italian study site” (D_5.2.2), which is part of the Activity 5.2 “Venice plan of adaptation” included in WP5 “Transferring”.

The goal of Activity 5.2 is to develop an original vulnerability map of the MoST Italian study area, which was selected between the southern Venice lagoon border and the final stretch of the Adige River.

In particular, the CNR contribution to the deliverable D_5.2.2 consisted in the following:

- Hydrogeological conceptualization of the vulnerability of farmlands to saltwater intrusion.
- Selection of proper indicators.
- Preparation of the layers related to the hydro-geo-morphological characteristics and of those describing the saltwater-freshwater setting in shallow aquifer and land subsidence processes.
- Assessment of the sensitivity, hazard and vulnerability maps.

This analysis performed within the MoST project proposes an update of the assessment of the vulnerability to saltwater intrusion previously provided by Da Lio *et al.*, 2015, on the basis of an improved concept of vulnerability and a wider dataset of environmental indicators.

The concept of vulnerability adopted in the MoST project (Tosi et al., 2022) refers to the propension of farmland systems to be negatively affected by saltwater intrusion, due to the intrinsic sensitivity of the system, when different triggers modify the present hazard status. Intrinsic sensitivity characteristics and present hazard status are described basing on relevant indicators accurately selected (i.e., fresh-saltwater interface depth, electrical resistivity of the

shallow subsoil, distance from salt- and freshwater sources, ground elevation, permeability of the shallow subsoil, potential runoff, land subsidence and sea-level rise) and then combined following an index-based approach.

2 The vulnerability analysis of farmland to saltwater intrusion: The MoST approach

The MoST vulnerability approach assumes that the farmland system vulnerable to the saltwater intrusion is the subsoil including the agricultural zone and the underneath layers up to 3-4 m depth (Tosi et al., 2022).

The vulnerability of farmlands to saltwater intrusion is characterized by combining the modelling of the present hazard status with a suite of relevant indicators potentially concurring to modify the magnitude of the overall vulnerability.

All data used in this work were already available from previous published studies and websites. Dataset, methods, indicators, and data sources used in the vulnerability assessment are summarized in Table 3.

In order to assess the vulnerability of the coastal farmlands to saltwater intrusion, SIN and AER thematic layers, representing the present hazard status, were combined with all the intrinsic sensitivity indicators, i.e. SAD, FRD, PER, ROF, and RGLC, which potentially can alter the present status increasing the overall vulnerability (Table 3).

Haz	Indicators	Dataset	Method	Data source

	Saline interface depth (SIN)	Electrical resistivity	Airborne Electromagnetic	(Tosi *et al.*, 2018)
	Electrical resistivity of the uppermost subsoil layer (AER)			
Sensitivity	Distance from salt- (SAD) and freshwater sources (FRD)	Spatial information	Satellite images	Google Earth, 2021
	Ground elevation (GEL)	Digital Terrain Model	Lidar	Regione del Veneto
	Permeability of the shallow aquifer (PER)	Permeability of the shallow subsoil	Agriculture and pedology	ARPAV
		Geomorphological map	Geology, Sedimentology, Geomorphology	Città Metropolitana di Venezia
	Potential runoff (ROF)	Hydrologic Soil Groups	Agriculture and pedology	ARPAV
	Relative ground level change (RGLC)	Ground displacements	SAR interferometry	(Tosi *et al.*, 2020)
		Sea-level time series	Tide gauge time series	(Zanchettin *et al.*, 2021)

Table 1 - Sensitivity/Hazard status indicators and available dataset used in the vulnerability assessment.

The modelling approach is summarized in Fig. 3 and described in the following.

- Relevant indicators were selected and the corresponding dataset were gridded on a 5-m regular cell grid using the kriging method (Cressie, 1990), resulting in a total of 7767096 nodes for each thematic layer.
- Each layer was classified into five intervals of increasing importance with respect to its contribution to sensitivity or hazard status. Maximun and minumun boundaries between classes were chosen based on previous investigations (de Franco *et al.*, 2009; Viezzoli *et al.*, 2010; Da Lio *et al.*, 2015; Tosi *et al.*, 2018). The intermediate limits were instead defined by analyzing the nodes frequency distribution and classifying them through an equal area criterion.
- In order to create homogenous ranking between different layers, a score, ranging between 0 and 4, was assigned to each class representing the increasing contribution to the vulnerability of the system.
- The sensitivity map was estimated according to the following equation (2):

$$Sensitivity = \frac{\sum_{i=1}^{n} \omega_i I_i}{\sum_{i=1}^{n} \omega_i} \qquad \text{(Equation 1)}$$

- where the n sensitivity indicators (I) (i.e. SAD, FRD, PER, ROF, and RGLC) were weighted (ω) by using pairwise comparisons following the AHP approach (Saaty, 1990, 2003), a technique developed for multicriteria decision making problems. AHP is a scaling method to be applied to prioritized indicators, where relative scales are derived using expert judgements given in the form of pairwise comparisons. The AHP analysis was performed using the R-package ahpsurvey package (v. 0.4.1) by Cho, 2019. The AHP also provides a mathematical measure to determine the consistency of judgments. The coherence of the pair-wise comparisons is calculated to ensure the proportionality and transitivity of the results by calculating the consistency ratio (Cr), as defined by (Saaty,

1990), which also suggest that Cr of the order of 0.1 or less is considered to be a reasonable level of consistency (Saaty, 1990).

- The vulnerability map will be then computed by combining the sensitivity map with the present hazard status following the equation (3):

$$Vulnerability = Sensitivity + Hazard\ status \qquad \textit{(Equation 2)}$$

Three different hazard status were considered: (i) SIN, (ii) AER, and (iii) their combination SIN&AER.

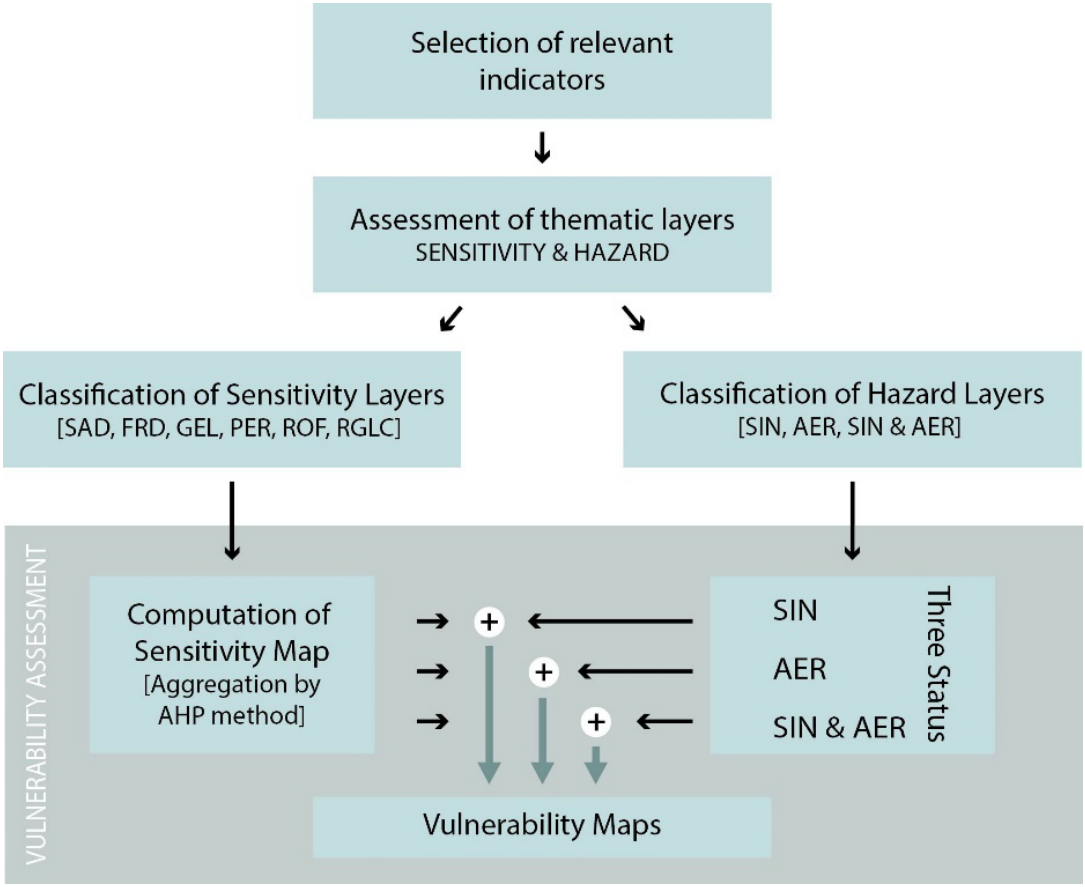

Fig. 1 – Workflow of the approach adopted to compute vulnerability maps (Tosi et al., 2022).

3 Results

3.1 Sensitivity layer classification

The classification of salt- and freshwater distance thematic layers (SAD and FRD) was based on the expected effect of salinization/freshening of the subsoil by the nearby watercourses, as observed through the monitoring well networks and in the AEM data (de Franco *et al.*, 2009; Da Lio *et al.*, 2015; Tosi *et al.*, 2018). Overall, salt- and freshwater dispersion significantly decreases within some hundreds of meters from the source. The classification of distance adopted for saline watercourses was applied also to seashore and lagoon margins, affected by surficial infiltration of saltwater due to storm surges. The minimum and maximum distances considered in the classification of SAD and FRD are 100 and 800 m (Fig. 4).

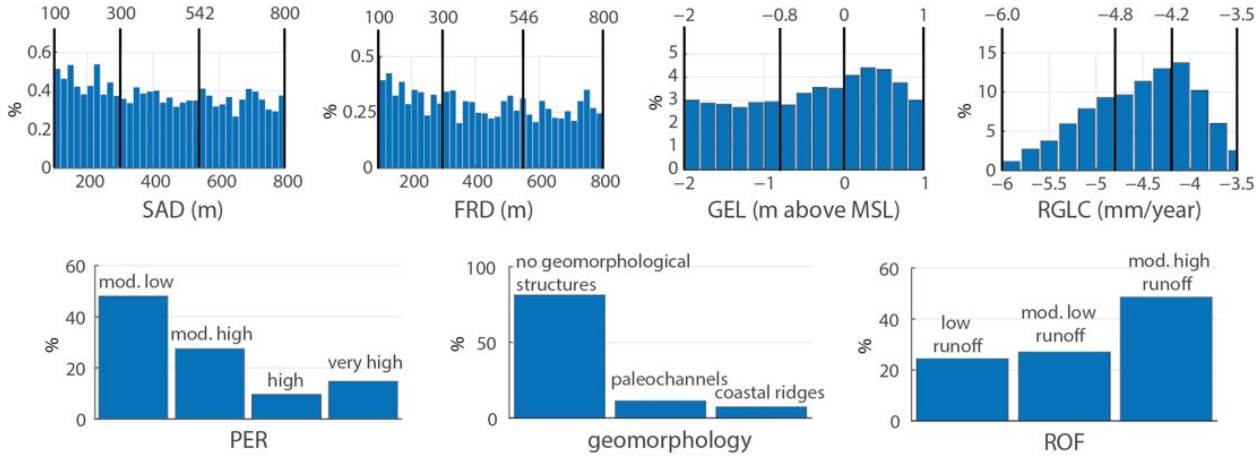

Fig. 2 – Frequency distribution of each sensitivity layer in the dataset (i.e., percentage of nodes in each thematic layer class over the total amount of nodes considered in the study area) confined within the minimum and the maximum boundaries set for scores 0 and 4, respectively. The abbreviation mod. means moderately, the acronym MSL means mean sea level (Tosi et al., 2022).

Ground elevation level is considered to highly influence salinization processes since a large part of the study area lies below the mean sea level and without the artificial management of the water table, most of the coastland would be naturally flooded by the sea. Locally, freshwater lenses could develop in the surficial aquifer where the ground elevation is above the mean sea level (e.g., in the littoral sector). Therefore, areas with ground level higher than 1 m above msl are assumed to be negligibly sensitive to the salinization process, while those lying below -2 m were given the highest importance.

The classification of the permeability and potential runoff layers was primarily based on the original classification (ARPAV, 2011). Considering that geomorphological structures, such as paleochannels and coastal ridges, act as preferential pathways for saltwater intrusion, the information obtained from the geomorphological map were combined with the PER layer. In particular, each PER class was increased by one (e.g., class 1 was raised to class 2) wherever a buried permeable sedimentary body occurred. Overall, about 19% of the study area changed to a worse class due to this effect (Fig. 4).

For the classification of the relative ground level change, which results from the land subsidence increased by the sea-level rise, the values of -3.5 mm/yr and -6 mm/yr were used for defining the lowest and highest classes of importance, respectively. Within this range about 97% of the study area is included (Fig. 4).

The intermediate limits, classified through an equal area criterion of the nodes' distribution, are shown in Table 4, which reports the ranges and scores of the thematic layer classification (Fig. 4). Once the sensitivity layers were classified, a score from 0 to 4 was assigned going from low to high contribution to vulnerability, in accordance with several methods available in the literature (e.g.,Gorgij & Moghaddam, 2016; Azizi et al., 2019; Kazakis et al., 2019). Fig. 5 shows the results of the classification of each thematic layer in the study area with color-coding highlighting the rating in accordance with the classification shown in Table 4.

SAD m	FRD m	GEL m above msl	PER mm/h	ROF	RGLC mm/yr	Score
>800	<100	>1	moderately low 0.36 – 3.6	Low	>-3.5	**0**
546 – 800	100 – 300	0.0 – 1.0	moderately high 3.6 – 36		-4.2 – -3.5	**1**
300 – 546	300 – 542	-0.8 – 0.0	high 36 – 360	moderately low	-4.8 – -4.2	**2**
100 – 300	542 – 800	-2.0 – -0.8	very high >360		-6.0 – -4.8	**3**
<100	>800	<-2.0	n.p.	moderately high	<-6.0	**4**

Table 2 – Sensitivity layer classification: ranges and scores. The values of 0 and 4 represent low and high contribution to vulnerability, respectively. To note that PER ranking is increased of one score in correspondence of geomorphological structures.

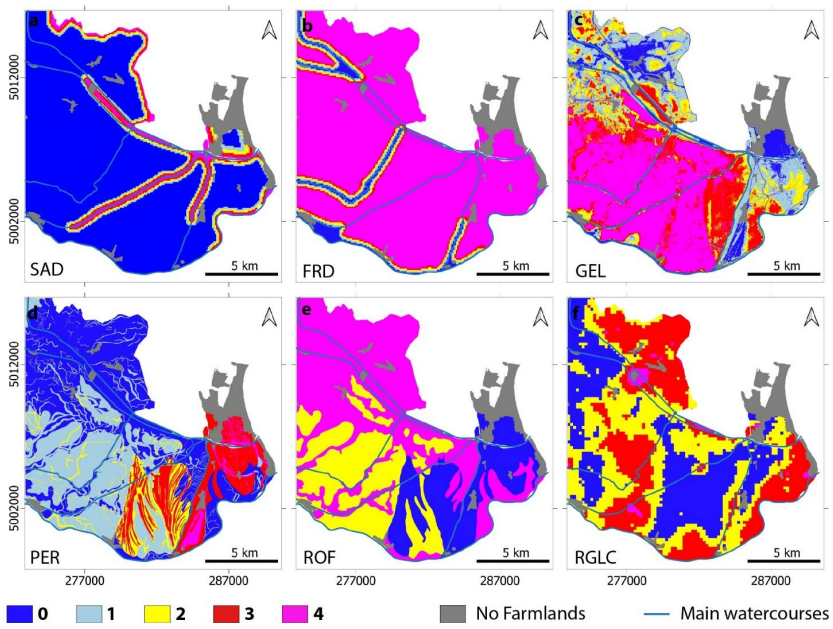

Fig. 3 – Classification of the sensitivity layers: a) saltwater distance (SAD), b) freshwater distance (FRD), c) ground elevation level (GEL), d) permeability (PER), e) potential runoff (ROF), and f) relative ground level change (RGLC). Scores from 0 to 4 identify low to high contributions to vulnerability. To note that PER layer combines permeability and geomorphological structures (Tosi et al., 2022).

3.2 Hazard layer classification

The present status of the salinity hazard is described by the magnitude of the salinization process in relation to the farmland systems. The magnitude was retrieved by the AEM survey reaching almost 100 m depth below the ground level, in terms of electrical resistivity sections, here used as an indirect measurement of the subsoil salinity. Therefore, the two indicators obtained by AEM dataset, i.e. the depth of the fresh- saltwater interface and the average electrical resistivity of the shallow subsoil, were selected to describe the actual salinization state of the farmland systems.

The hazard layers (i.e. SIN, AER, and their combination SIN&AER) were categorized into five classes with respect to their contribution to vulnerability, with progressively increasing importance, following the same criteria adopted for the classification of the sensitivity layers.

For the saline interface depth, the highest level of hazard is assumed to be at a depth lower than 1.5 m, in order to account for the seasonal variations of the water table induced by hydraulic regulations. The lowest level of hazard was defined at a depth of 6 m below ground, reasonably assumed as the maximum depth where land reclamation activities and climate changes have acted, at least over a decade.

Maximum and minimum values of the average electrical resistivity hazard of the shallow subsoil were set at values of 2 Ωm and 10 Ωm, respectively. In fact, based on monitoring wells data (Carbognin & Tosi, 2003; de Franco et al., 2009), these resistivity values generally refer to a groundwater salinity of approximately 30-35 g/l and 3-5 g/l.

When considering the average electrical resistivity combined with the saline interface depth, the five AER classes were combined with only the SIN classes belonging to the depth interval 0 – 1.5 m representing the agricultural zone. The frequency distribution of the nodes of the thematic layers and the thematic layer classification are shown in Fig. 6 and Table 5, respectively.

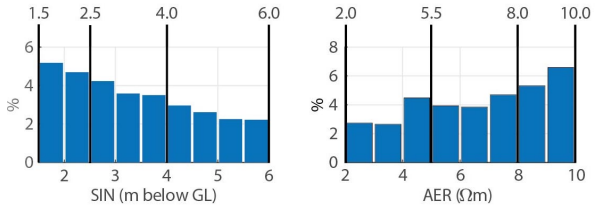

Fig. 4 – Frequency distribution of the dataset in each hazard layer (i.e., percentage of nodes in each thematic layer class over the total amount of nodes considered in the study area) confined within the minimum and the maximum boundaries set for score 0 and 4, respectively. The acronym GL means ground level (Tosi et al., 2022).

SIN m below GL	AER Ωm	Score
>6.0	>10.0	**0**
4.0 – 6.0	8.0 – 10.0	**1**
2.5 – 4.0	5.5 – 8	**2**
1.5 – 2.5	2.0 – 5.5	**3**
<1.5	<2.0	**4**

Table 3 – Hazard layer classification: ranges and scores. The values of 0 and 4 mean low and high contribution to vulnerability, respectively.

The classified hazard layers are reported in Fig. 7. The map obtained by SIN depicts a general variability of the hazard classes with the worse conditions in the sectors close to the lagoon margin and in some inner areas (Fig. 7a). Regarding the hazard mapped by the AER, it shows 0-score extent for the most part of the study area and it increases to the highest 4-score only close to the lagoon margin (Fig. 7b). The combined threat of SIN and AER highlights a general decrease hazard condition when considering high scores of SIN combined with low scores of AER in the uppermost soils (Fig. 7c).

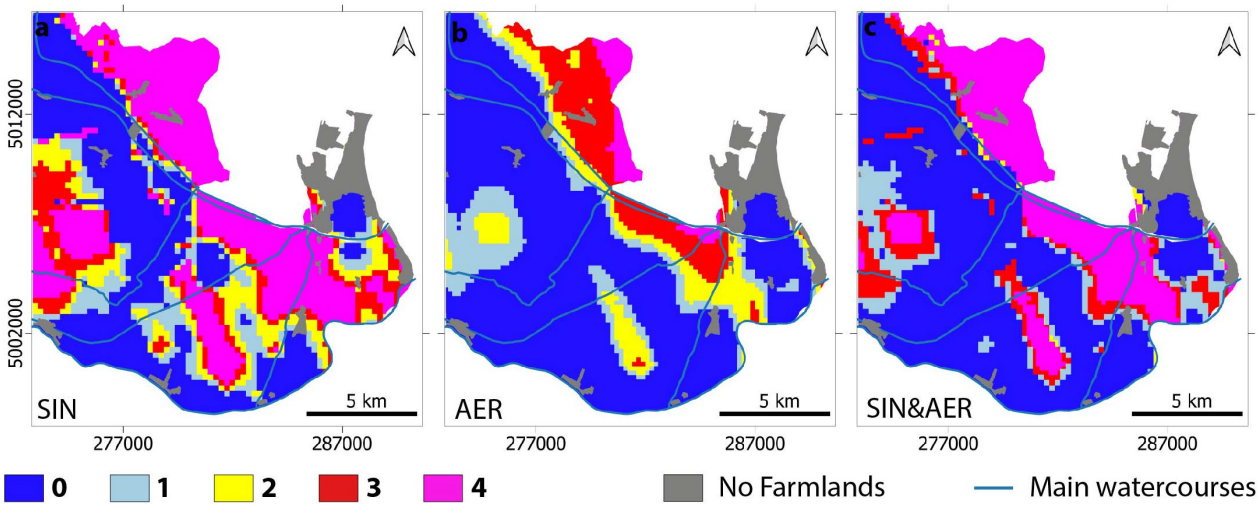

Fig. 5 – Classification of the hazard layers: a) fresh-saltwater interface depth (SIN), b) average electrical resistivity (AER), and c) fresh-saltwater interface depth (SIN) combined with average electrical resistivity (SIN&AER). Scores from 0 to 4 identify low to high contributions to vulnerability (Tosi et al., 2022).

3.3 Sensitivity set up of the farmland system

The sensitivity map was obtained by combining the classified sensitivity layers according to equation (2). The AHP process (Saaty, 1990) has been implement using through the judgments of six experts in different disciplines related to the saltwater intrusion in coastal areas (e.g., hydrogeology, stratigraphy, oceanography) by compiling a pairwise comparison matrix for the sensitivity indicators.

The individual preference weights were computed using the Dominant Eigenvalue method described in (Saaty, 2003) and were then aggregated by arithmetic averaging. A certain degree of heterogeneity resulted, despite the six expert judgements were consistent, with an overall

mean consistence ratio Cr=0.03 well below the suggested threshold (one case exhibiting Cr=0.1, red dots; the remaining 5 cases being largely <0.1).

The resulting weights (Table 6) allow to rank the factors with respect to their expected contribution in the sensitivity computation. The weight of ground elevation results the highest, almost double than the relative ground level change, whereas the other contributions are significantly lower.

Sensitivity indicators	**Weight**		
	mean	**st.dev**	**(%)**
SAD	0.117	0.06	11.7
FRD	0.084	0.07	8.4
GEL	0.373	0.14	37.3
RGLC	0.208	0.06	20.8
PER	0.145	0.09	14.5
ROF	0.073	0.01	7.3

Table 4 – Weights assigned to each sensitivity indicator resulting from the AHP process.

The resulting sensitivity map (Fig. 8) shows a high heterogeneity in the distribution of the sensitivity classes, which emphasize the geomorphological conditions of the study area, i.e. the ground elevation and the presence of the buried sand bodies. Extreme and negligible sensitivity classes are limited in extent and generally correspond to narrow strips along the Gorzone Channel, Brenta and Bacchiglione rivers, and in the inner part of the coastal ridges. Sectors with marginal to strong sensitivity classes are almost evenly distributed and cover most of the central area.

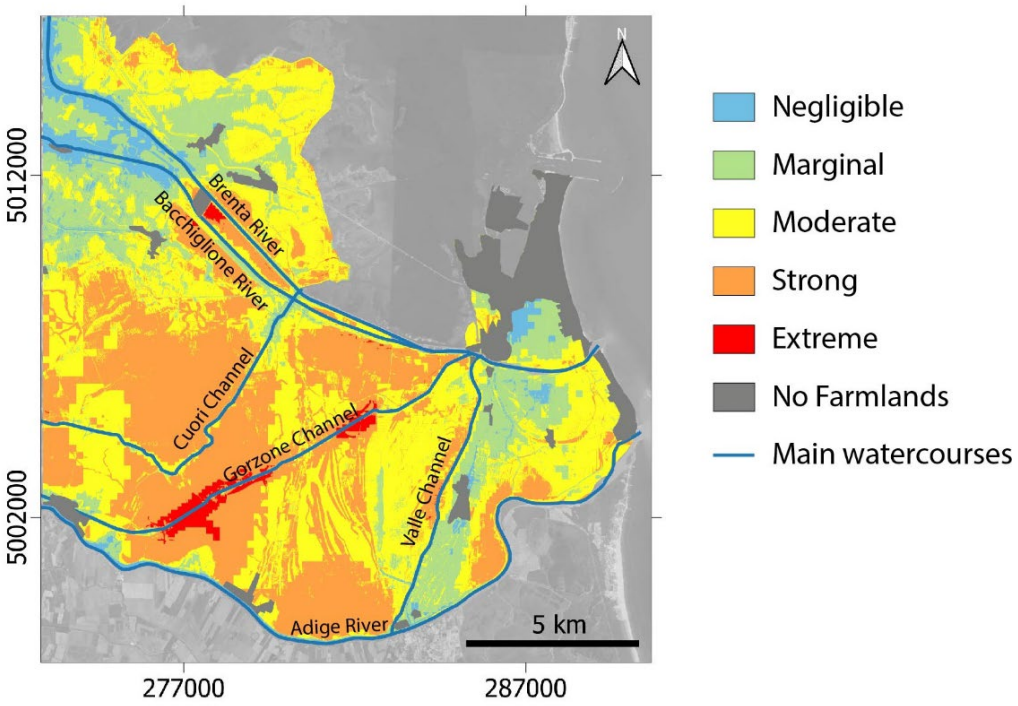

Fig. 6 – Map of sensitivity of farmlands to saltwater intrusion. The map was computed accounting for the sensitivity indicators: SAD, FRD, GEL, RGLC, PER, ROF (Tosi et al., 2022).

3.4 Vulnerability Analysis of the Farmland System

According to the adopted procedure, three vulnerability maps were produced (Fig. 8). Vulnerabilities are described by five classes: negligible, marginal, moderate, strong, and extreme. Specifically, the vulnerability is investigated by considering three hazard statuses. The first and second statuses separately account for the indicators representing the depth of the freshwater–saltwater interface and the average electrical resistivity of the shallow subsoil. The third one combines the former status to capture the threat of the resistivity in specific sectors of the farmlands where the saline interface is at depths lower than 1.5 m below the ground.

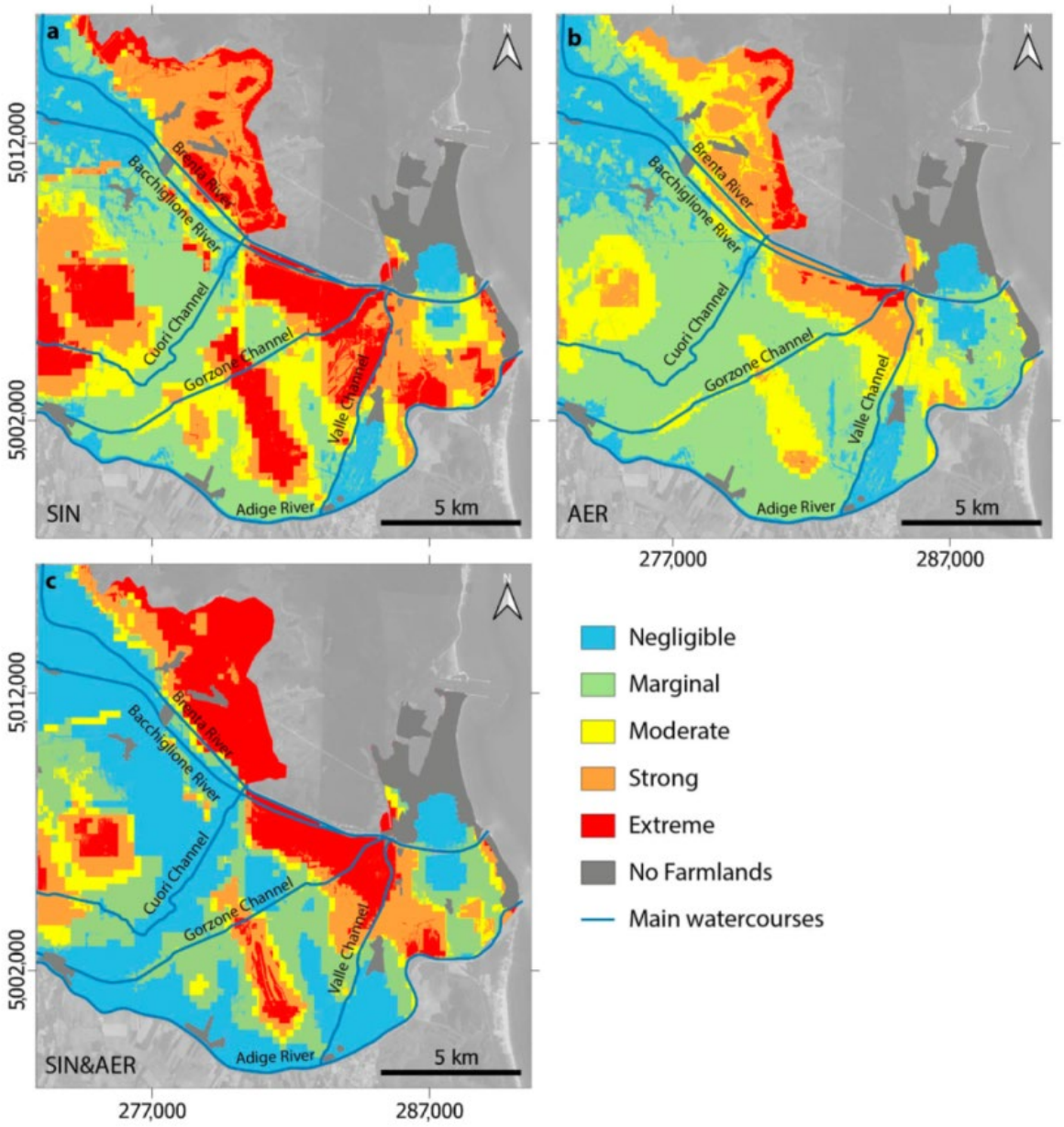

Fig. 7 – Map of the vulnerability of farmlands to saltwater intrusion. The maps were computed while accounting for the sensitivity of the farmlands and the three hazard statuses: (a) SIN hazard, (b) AER hazard, and (c) SIN&AER hazard. Coordinate system: UTM33, WGS84 (Tosi et al., 2022).

The vulnerability map, computed by considering the SIN-hazard status, results in rather equally spatially distributed classes, covering 15% to 25% of the area. Conversely, in the vulnerability maps computed by considering AER- and SIN&AER-hazard statuses, the marginal (46%) and negligible (41%) classes prevail, respectively. All the vulnerability maps are clearly a signature of the considered hazard status. Interestingly, strong-to-extreme classes occur in specific areas for all the vulnerability maps. In detail, lagoon borders, the littoral at the Brenta–Bacchiglione river mouth, the seaward portion of the Adige river, and some local sectors up to 10–15 km inland exhibit the highest scores. Similarly, some areas fall into the negligible class in all the vulnerability maps, e.g., the area of Sottomarina, the northwestern inland between the Brenta and the Bacchiglione rivers, and the right side of the Valle channel.

4 Final remarks

This work proposed an assessment of the vulnerability of the Venice coastland farmlands to saltwater intrusion by combining the intrinsic sensitivity characteristics with the present hazard status of salinization. An important point to be considered in the analysis of the vulnerability to saltwater intrusion is the definition of the environmental target. Clearly, the vulnerability analysis of the aquifer is different from that of the farmlands. In addition, a specific model of farmland system must be conceptualized according to the boundary conditions.

In this study, the farmland system that is likely vulnerable to the saltwater intrusion is assumed to be the subsurface layer that includes the agricultural zone and the underneath shallow subsoil up to 3–4 m depth, where saltwater intrusion may threaten agricultural productivity. The sensitivity to saltwater intrusion was set up by aggregating six physical indicators that potentially

concur to intensify or mitigate salinization effects on the farmland system. The aggregation was computed by using pairwise comparisons among the indicators, following the AHP approach.

Regarding the salinization status, a new approach was defined for delineating the saline-hazard status on the system. The approach consisted of considering the freshwater–saltwater interface depth and the average electrical resistivity of the shallow subsoil, firstly as separate indicators of hazard status, and then as combined factors. Looking at the SIN and AER hazard status, we see that farmlands should be strongly affected by saltwater intrusion where the freshwater–saltwater interface rises close to agricultural soil and high AER values occur. However, our SIN- and AER-hazard comparison shows rather opposite conditions in some areas. For this reason, the SIN&AER was deemed to be more representative of the farmland-system hazard status than those computed by considering the indicators separately. In fact, according to our definition of farmland system, the vulnerability assessment computed by using the SIN-hazard status is likely overestimated with respect to that of AER-hazard status. Meanwhile, the use of the SIN&AER-hazard status permits us to adjust some classes apparently over- or underestimated by hazard status, based on SIN and AER separately. For example, the northern area bounding the lagoon margin increases in vulnerability when moving from the strong to extreme class, while the inner region behaves oppositely, and vulnerability decreases from the strong to the negligible class. Consequently, the contrast on the map is enhanced, and buffering zones of smooth transition between intermediate and extreme vulnerability are absent. SIN&AER is more coherent with AER where vulnerability is low (about 12,000 hectares); vice versa, it is more coherent with SIN where vulnerability is extreme (about 6000 hectares). This means that the remaining 10% of the study area is in the intermediate-vulnerability class.

A comparison between the three vulnerability maps is reported in Fig. 8. A rather equal spatial distribution of the vulnerability classes results by considering the SIN-hazard status, covering 15%

to 25% of the area. Conversely, the marginal (46%) and negligible (41%) classes prevail when using the AER- and SIN&AER-hazard statuses.

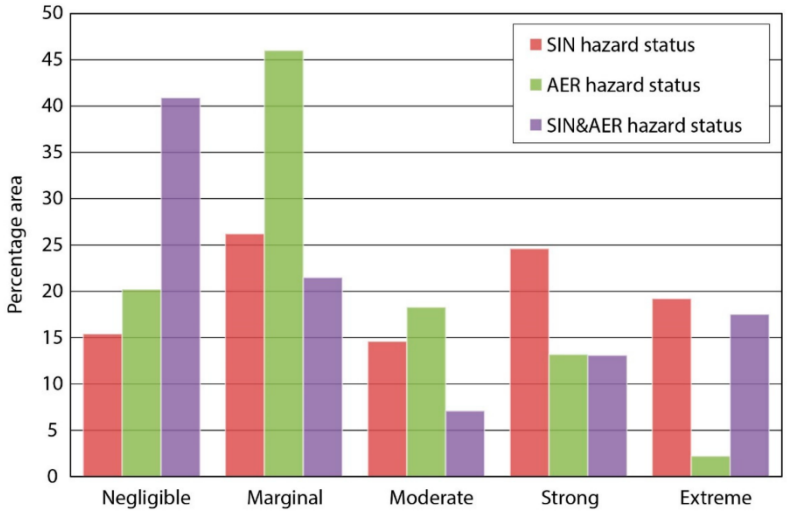

Fig. 8 – Areal extent of vulnerability classes (%) for the three hazard statuses (Tosi et al., 2022).

Concluding, the main outcomes of this activity can be summarized as follows.

- The combined hazard map of freshwater–saltwater interface depth and average electrical resistivity allowed the authors to capture the salinization threat on the agricultural zone without neglecting that on the underlying shallow subsoil. The vulnerability maps that were obtained by considering the two hazard statuses separately depict a less realistic representation of the fragilities of the farmland system, while their combination adjusts some classes apparently over-/underestimated.
- The vulnerability of Venice farmland system is in the strong and extreme classes in about 30% of the area, marginal and moderate in the 28%, and negligible in the 40%.

- The outcomes of this research, compared with the previous assessments, confirm the heterogeneous distribution of the vulnerability in the study area. However, the differences between the two maps should be cautiously interpreted, because they focus on different targets, characterization of the sensitivity of the farmland system, and conceptualization of the hazard status.

5 References

ARPAV (2011) Valutazione della permeabilità e del gruppo idrologico dei suoli del Veneto. 1–19 pp.

Azizi, F., Vadiati, M., Asghari, A., Amirhossein, M. and Jan, N. (2019) A hydrogeological-based multi-criteria method for assessing the vulnerability of coastal aquifers to saltwater intrusion. *Environ. Earth Sci.*, 78, 548.

Carbognin, L. and Tosi, L. (2003) Il progetto ISES per l'analisi dei processi di intrusione salina e subsidenza nei territori meridionali delle provincie di Padova e Venezia. 95 pp.

Carver, S.J. (1991) Integrating multicriteria evaluation with Geographical Information Systems. *Int. J. Geogr. Inf. Syst.*, 5, 321–339.

Cho, F. (2019) Analytic Hierarchy Process for Survey Data in R Vignettes for the ahpsurvey package (ver 0.4.1). 24 pp.

Cressie, N. (1990) The origins of kriging. *Math. Geol.*, 22, 239–252.

Da Lio, C., Carol, E., Kruse, E., Teatini, P. and Tosi, L. (2015) Saltwater contamination in the managed low-lying farmland of the Venice coast, Italy: An assessment of vulnerability. *Sci.*

Total Environ., 533, 356–369.

de Franco, R., Biella, G., Tosi, L., Teatini, P., Lozej, A., Chiozzotto, B., Giada, M., Rizzetto, F., Claude, C., Mayer, A., Bassan, V. and Gasparetto-Stori, G. (2009) Monitoring the saltwater intrusion by time lapse electrical resistivity tomography: The Chioggia test site (Venice Lagoon, Italy). *J. Appl. Geophys.*, 69, 117–130.

Gorgij, A.D. and Moghaddam, A.A. (2016) Vulnerability Assessment of saltwater intrusion using simplified GAPDIT method: a case study of Azarshahr Plain Aquifer, East Azerbaijan, Iran. *Arab. J. Geosci.*, 9, 106.

Kazakis, N., Busico, G., Colombani, N., Mastrocicco, M., Pavlou, A. and Voudouris, K. (2019) GALDIT-SUSI a modified method to account for surface water bodies in the assessment of aquifer vulnerability to seawater intrusion. *J. Environ. Manage.*, 235, 257–265.

Saaty, T.L. (1990) How to make a decision: The analytic hierarchy process. *Eur. J. Oper. Res.*, 48, 9–26.

Saaty, T.L. (2003) Decision-making with the AHP: Why is the principal eigenvector necessary. *Eur. J. Oper. Res.*, 145, 85–91.

Tosi, L., Carbognin, L., Teatini, P., Rosselli, R., Gasparetto Stori, G. The ISES Project subsidence monitoring of the catchment basin south of the Venice Lagoon (Italy). In Land subsidence: Proceedings of the Sixth International Symposium on Land Subsidence, Ravenna, Italy, 24–29 September 2000; CNR, Grupo Nazionale per la Difesa dalle Catastrofi Idrogeologiche: Venice, Italy, 2000; Volume 2, pp. 113–126.

Tosi, L., Da Lio, C., Donnici, S., Strozzi, T. and Teatini, P. (2020) Vulnerability of Venice's coastland to relative sea-level rise. *Proc. Int. Assoc. Hydrol. Sci.*, 382, 689–695.

Tosi, L., Da Lio, C., Teatini, P., Menghini, A. and Viezzoli, A. (2018) Continental and marine surficial water - Groundwater interactions: The case of the southern coastland of Venice (Italy). *Proc. Int. Assoc. Hydrol. Sci.*, 379, 387–392.

Tosi, L., Da Lio., C, Bergamasco, A., Cosma, M., Cavallina, C., Fasson, A., Viezzoli, A., Zaggia, L., Donnici, S. (20122) Sensitivity, Hazard, and Vulnerability of Farmlands to Saltwater Intrusion in Low-Lying Coastal Areas of Venice, Italy. *Water*. 2022; 14(1):64. https://doi.org/10.3390/w14010064

Viezzoli, A., Tosi, L., Teatini, P. and Silvestri, S. (2010) Surface water-groundwater exchange in transitional coastal environments by airborne electromagnetics: The Venice Lagoon example. *Geophys. Res. Lett.*, 37, L01402.

Zanchettin, D., Bruni, S., Raicich, F., Lionello, P., Adloff, F., Androsov, A., Antonioli, F., Artale, V., Carminati, E., Ferrarin, C., Fofonova, V., Nicholls, R.J., Rubinetti, S., Rubino, A., Sannino, G., Spada, G., Thiéblemont, R., Tsimplis, M., Umgiesser, G., Vignudelli, S., Wöppelmann, G. and Zerbini, S. (2021) Sea-level rise in Venice: Historic and future trends (review article). *Nat. Hazards Earth Syst. Sci.*, 21, 2643–2678.